FOURTH EDITION



# NUCLEAR CARDIOLOGY

## PRACTICAL APPLICATIONS



GARY V. HELLER
ROBERT C. HENDEL

Mc Graw Hill

# Nuclear Cardiology

## Notice

Medicine is an ever-changing science. As new research and clinical experience broaden our knowledge, changes in treatment and drug therapy are required. The authors and the publisher of this work have checked with sources believed to be reliable in their efforts to provide information that is complete and generally in accord with the standards accepted at the time of publication. However, in view of the possibility of human error or changes in medical sciences, neither the authors nor the publisher nor any other party who has been involved in the preparation or publication of this work warrants that the information contained herein is in every respect accurate or complete, and they disclaim all responsibility for any errors or omissions or for the results obtained from use of the information contained in this work. Readers are encouraged to confirm the information contained herein with other sources. For example, and in particular, readers are advised to check the product information sheet included in the package of each drug they plan to administer to be certain that the information contained in this work is accurate and that changes have not been made in the recommended dose or in the contraindications for administration. This recommendation is of particular importance in connection with new or infrequently used drugs.

# Nuclear Cardiology

## Practical Applications

**Fourth Edition**

**Gary V. Heller, MD, PhD, MASNC, FACC**

Gagnon Cardiovascular Institute
Morristown Medical Center
Morristown, New Jersey

**Robert C. Hendel, MD, MACC, MASNC, FAHA, FSCCT**

Sidney W. and Marilyn S. Lassen Chair in Cardiovascular Medicine
Professor of Medicine and Radiology
Tulane University School of Medicine
New Orleans, Louisiana


New York Chicago San Francisco Athens London Madrid Mexico City
Milan New Delhi Singapore Sydney Toronto

ISBN: 978-1-26-425721-8
MHID: 1-26-425721-X

The material in this eBook also appears in the print version of this title: ISBN: 978-1-26-425720-1,
MHID: 1-26-425720-1.

eBook conversion by codeMantra
Version 1.0

*This edition is dedicated to the readers who will find this edition useful as this has been the goal of our efforts to complete this revision, especially an era of COVID where everything has been more difficult, but new important knowledge has been emerging and important. I primarily dedicate this to my co-editor, friend and colleague, Bob Hendel, who has had such an important role in all four editions bringing important comments, revisions, and humor to the process.*

G.V.H.

*For my colleagues-past, present, and future, who have provided me with inspiration throughout my career. Additionally, this book is also dedicated to those "behind the scenes," such as our dedicated and passionate technologists, thoughtful administrators, and societal/regulatory personnel who help optimize the value of nuclear cardiology. And of course, to Gary Heller, the instigator and inspirator for* Nuclear Cardiology: Practical Applications *and kayaker extraordinaire.*

R.C.H.

*This page intentionally left blank*

# CONTENTS


**Contributors** . . . . . ix

**Preface** . . . . . xiii

**Section 1. Fundamentals of Nuclear Cardiology** . . . . . 1

1. **Fundamentals of Nuclear Cardiology Physics** . . . . . 3
   C. David Cooke, James R. Galt and E. Lindsey Tauxe
2. **Radiation Safety and Protection in Nuclear Cardiology** . . . . . 15
   James R. Galt, C. David Cooke and Jason S. Tavel
3. **Radiopharmaceuticals for Cardiovascular Imaging** . . . . . 29
   James A. Case and Gary V. Heller
4. **Cardiac SPECT and PET Instrumentation** . . 49
   James A. Case
5. **Quality Control in SPECT, Dedicated PET, and Hybrid CT Imaging** . . . . . 73
   Sue Miller, Sunil Selvin and Joey Stevens
6. **Radiation Exposure and Reduction Strategies in Myocardial Perfusion Imaging** . . . . . 97
   Michael C. Desiderio and Gary V. Heller
7. **Physician Certification and Laboratory Accreditation** . . . . . 109
   Robert C. Hendel and Gursukhman Deep S. Sidhu

**Section 2. Radionuclide Myocardial Perfusion Imaging** . . . . . 119

8. **Exercise and Pharmacologic Stress Testing** . . . . . 121
   Seyed Mehdi Khalafi, Archana Ramireddy and Robert C. Hendel
9. **SPECT Myocardial Perfusion Imaging Protocols** . . . . . 141
   Milena J. Henzlova, Cole B. Hirschfeld and Andrew J. Einstein
10. **Cardiovascular Positron Emission Tomographic Imaging** . . . . . 155
    Matthew J. Memmott, Parthiban Arumugam and Gary V. Heller
11. **Myocardial Blood Flow Quantitation in Clinical Practice** . . . . . 175
    Krishna K. Patel, Gary V. Heller and Timothy M. Bateman
12. **Ventricular Function** . . . . . 195
    Prem Soman and Saurabh Malhotra
13. **Non-Cardiac Findings** . . . . . 217
    Rupa M. Sanghani and Jamario Skeete
14. **Interpretation and Reporting of SPECT and PET Myocardial Perfusion Imaging** . . . 233
    Robert C. Hendel and Gary V. Heller

**Section 3. Indications and Applications** . . . . . 271

15. **Clinical Applications of Quantitation and Artificial Intelligence in Nuclear Cardiology** . . . . . 273
    Robert J.H. Miller and Piotr J. Slomka
16. **Appropriate Use of Nuclear Cardiology Techniques** . . . . . 289
    Gursukhman Deep S. Sidhu and Robert C. Hendel
17. **Evaluation of Patients with Suspected Coronary Artery Disease** . . . . . 299
    Sanjeev U. Nair and Gary V. Heller
18. **Evaluation of Patients with Known Coronary Artery Disease** . . . . . 323
    Javier Gomez and Rami Doukky

**19. Risk Stratification with Myocardial Perfusion Imaging** . . . . . 339
Javier Gomez and Rami Doukky

**20. Nuclear Cardiovascular Imaging in Special Populations** . . . . . 371
Robert C. Hendel, Michael C. Desiderio and Gary V. Heller

**21. Preoperative Risk Assessment for Noncardiac Surgery** . . . . . 405
Muhammad Siyab Panhwar, Sumeet S. Mitter and Robert C. Hendel

**22. Radionuclide Imaging in Heart Failure** . . . 419
Gautam V. Ramani and Prem Soman

**Section 4. Beyond Perfusion Imaging** . . . . . 429

**23. Nuclear Cardiology Procedures in the Evaluation of Myocardial Viability** . . . . . 431
Christiane Wiefels, Fernanda Erthal, Benjamin Chow, Gary V. Heller and Rob S.B. Beanlands

**24. Radionuclide Imaging of Cardiac Innervation** . . . . . 457
Mark I. Travin and Ana Valdivia

**25. Imaging Cardiac Amyloidosis** . . . . . 479
Cory Henderson, Dillenia Rosica and Sharmila Dorbala

**26. $^{18}$F-FDG PET/CT for Imaging Cardiac Sarcoidosis and Inflammation** . . . . . 495
Cesia Gallegos, Bryan D. Young and Edward J. Miller

**27. Hybrid Imaging: SPECT–CT and PET–CT** . . 517
Cory Henderson, Patrycja Galazka and Sharmila Dorbala

**Section 5. Review Questions** . . . . . 533

**Answers and Explanations for Review Questions** . . . . . 563

**Index** . . . . . 585

# CONTRIBUTORS


**Parthiban Arumugam, MD**
Consultant Nuclear Medicine Physician and Clinical Director
Nuclear Medicine Centre
Manchester University NHS Foundation Trust
Manchester Royal Infirmary
Manchester, United Kingdom

**Timothy M. Bateman, MD**
Co-Director, Cardiovascular Radiologic Imaging
Saint-Lukes Health System
Professor of Medicine
University of Missouri-Kansas City
Kansas City, Missouri

**Rob S.B. Beanlands, MD, FRCPC, FCCS, FACC, FASNC**
Vered Chair and Head, Division of Cardiology
Professor, Medicine (Cardiology)/Radiology
Distinguished Research Chair University of Ottawa
Director, National Cardiac PET Centre
University of Ottawa Heart Institute
Ottawa, Ontario, Canada

**James A. Case, PhD, MASNC**
University of Missouri, Columbia
Chief Scientific Officer, Cardiovascular Imaging Technologies
Kansas City, Missouri

**Benjamin Chow, MD, FRCPC, FACC, FESC, FASNC, MSCCT**
Director of Cardiac Imaging
Saul & Edna Goldfarb Chair in Cardiac Imaging
Director of Cardiac Imaging Fellowship Training
Co-Director of Cardiac Radiology
Professor, Departments of Medicine (Cardiology) and Radiology
University of Ottawa Heart Institute
Ottawa, Ontario, Canada

**C. David Cooke, MSEE**
Lead Applications Developer/Analyst
Department of Radiology and Imaging Sciences
Emory University School of Medicine
Atlanta, Georgia

**Michael C. Desiderio, DO, FACC**
Medical Director, Cardiology
UPMC North Central Pennsylvania Region
Williamsport, Pennsylvania

**Sharmila Dorbala, MD, MPH, FACC, MASNC**
Director of Nuclear Cardiology
Professor, Department of Radiology
Division of Nuclear Medicine and Molecular Imaging and the Noninvasive Cardiovascular Imaging Program
Heart and Vascular Center
Departments of Radiology and Medicine (Cardiology)
Brigham and Women's Hospital
Harvard Medical School
Boston, Massachusetts

**Rami Doukky, MD, MSc, MBA, FACC, FASNC**
Professor of Medicine and Radiology
Chairman, Division of Cardiology
Cook County Health
Chicago, Illinois

**Andrew J. Einstein, MD, PhD, FACC, FAHA, MASNC, MSCCT, FSCMR**
Associate Professor of Medicine (in Radiology)
Director, Nuclear Cardiology, Cardiac CT, and Cardiac MRI
Director, Advanced Cardiac Imaging Fellowship
Seymour, Paul and Gloria Milstein Division of Cardiology, Department of Medicine, and Department of Radiology
Columbia University Irving Medical Center/New York-Presbyterian Hospital
New York, New York

**Fernanda Erthal, MD**
Cardiac Imaging Staff
Department of Cardiac Imaging
Diagnosticos da America SA (DASA)
Rio de Janeiro, Brazil

**Patrycja Galazka, MD**
Fellow, Noninvasive Cardiovascular Imaging
The Noninvasive Cardiovascular Imaging Program
Heart and Vascular Center
Departments of Radiology and Medicine (Cardiology)
Brigham and Women's Hospital
Harvard Medical School
Boston, Massachusetts

**Cesia Gallegos, MD, MHS**
Assistant Professor of Medicine (Cardiology)
Section of Cardiovascular Medicine
Yale University School of Medicine
New Haven, Connecticut

**James R. Galt, PhD**
Director of Nuclear Medicine Physics
Professor, Department of Radiology and Imaging Sciences
Emory University School of Medicine
Atlanta, Georgia

**Javier Gomez, MD, FACC, FASNC**
Assistant Professor of Medicine
Director and Cardio-Oncology Services
Division of Cardiology
Cook County Health
Chicago, Illinois

**Gary V. Heller, MD, PhD, FACC, MASNC**
Gagnon Cardiovascular Institute
Morristown Medical Center
Morristown, New Jersey

**Robert C. Hendel, MD, FAHA, FSCCT, MACC, MASNC**
Sidney W. and Marilyn S. Lassen Chair in Cardiovascular Medicine
Professor of Medicine and Radiology
Tulane University School of Medicine
New Orleans, Louisiana

**Cory Henderson, MD**
Assistant Professor of Medicine and Radiology
Division of Cardiovascular Medicine, Department of Medicine
Boston University School of Medicine
Boston, Massachusetts

**Milena J. Henzlova, MD**
Professor of Medicine (retired)
Mount Sinai School of Medicine
New York, New York

**Cole B. Hirschfeld**
Fellow, Cardiovascular Disease
Weill Cornell Medicine
NewYork-Presbyterian Hospital
New York, New York

**Seyed Mehdi Khalafi, MD**
Cardiovascular Medicine Fellow
Tulane University Medical Center
New Orleans, Louisiana

**Saurabh Malhotra, MD, MPH, FACC, FASNC**
Director of Advanced Cardiac Imaging
Cook County Health
Associate Professor of Medicine
Rush Medical College
Chicago, Illinois

**Matthew J. Memmott, MSc**
Consultant Medical Physicist
Nuclear Medicine Centre
Manchester University NHS Foundation Trust
Manchester, United Kingdom

**Edward J. Miller, MD, PhD, FASNC, FACC**
Associate Professor of Medicine (Cardiology) and Radiology & Biomedical Imaging
Yale University School of Medicine
Section of Cardiovascular Medicine
New Haven, Connecticut

**Robert J.H. Miller, MD, FRCPC, FACC**
Clinical Assistant Professor
Department of Cardiac Sciences
University of Calgary and Libin Cardiovascular Institute
Calgary, Alberta, Canada

**Sue Miller, CNMT**
Chief Operating Officer
Molecular Imaging Services, Inc.
Newark, Delaware

**Sumeet S. Mitter, MD, MSc**
Assistant Professor
Department of Medicine, Division of Cardiology
Icahn School of Medicine at Mount Sinai
New York, New York

**Sanjeev U. Nair, MBBS, MD, FACP, FACC, FSCAI**
Interventional Cardiologist
SN Cardiovascular Associates
Fort Worth, Texas

**Muhammad Siyab Panhwar, MD**
Cardiovascular Medicine Fellow
Tulane University Medical Center
New Orleans, Louisiana

**Krishna K. Patel, MD, MSc**
Assistant Professor of Medicine (Cardiology) and Population Health and Policy
The Zena and Michael A. Wiener Cardiovascular Institute
Blavatnik Women's Health Research Institute
Institute for Transformative Clinical Trials
Icahn School of Medicine at Mount Sinai
New York, New York

**Gautam V. Ramani, MD**
Associate Professor of Medicine
Division of Cardiovascular Medicine
University of Maryland
Baltimore, Maryland

**Archana Ramireddy**
Clinical Cardiac Electrophysiologist
Kaiser Permanente Northern California
Santa Clara, California

**Dillenia Rosica, MD**
Clinical Assistant Professor of Radiology
Department of Radiology
Geisinger Health System
Danville, Pennsylvania

**Rupa M. Sanghani, MD, FACC, FASNC**
Associate Professor of Medicine
Division of Cardiology
Rush University Medical Center
Chicago, Illinois

**Sunil Selvin, CNMT**
Vice President, Operations & Clinical Education
Molecular Imaging Service, Inc.
Newark, Delaware

**Gursukhman Deep S. Sidhu, MD**
Cardiologist
Cardiovascular Institute of the South
Lafayette, Louisiana

**Jamario Skeete, MD**
Cardiovascular Disease Fellow
Division of Cardiology, Department of Medicine
Rush University Medical Center
Chicago, Illinois

**Piotr J. Slomka, PhD**
Director of Innovations in Imaging, Cedars-Sinai
Professor of Medicine and Cardiology
Division of Artificial Intelligence in Medicine, Cedars-Sinai
Professor of Medicine, UCLA School of Medicine
Los Angeles, California

**Prem Soman, MD, PhD**
Professor of Medicine, and Clinical & Translational Science
University of Pittsburgh
Associate Chief, Cardiology
Director, Nuclear Cardiology and the Cardiac Imaging Fellowship
Director, Cardiac Amyloidosis Center
University of Pittsburgh Medical Center
Pittsburgh, Pennsylvania

**Joey Stevens, CNMT**
Senior Clinical Accounts Manager
Molecular Imaging Services, Inc.
Newark, Delaware

**E. Lindsey Tauxe, MEd, CNMT, FASNC**
Operations Director (Retired)
Medicine-Cardiovascular Disease
University of Alabama at Birmingham
Birmingham, Alabama

**Jason S. Tavel, PhD, DABR**
Medical Physicist
Astarita Associates, Inc.
Smithtown, New York
Adjunct Assistant Professor
Molloy College
Rockville Centre, New York

**Mark I. Travin, MD, FACC, MASNC**
Department of Radiology/Division of Nuclear Medicine
Director of Cardiovascular Nuclear Medicine
Montefiore Medical Center
Professor of Clinical Radiology and Clinical Medicine
Albert Einstein College of Medicine
Bronx, New York

**Ana Valdivia, MD**
Department of Radiology/Division of Nuclear Medicine
Montefiore Medical Center
Albert Einstein College of Medicine
Bronx, New York

**Christiane Wiefels, MD, MSc**
Assistant Professor of Medicine
Division of Nuclear Medicine, Department of Medicine
University of Ottawa
Ottawa, Ontario, Canada
PhD Candidate
Federal Fluminense University
Brazil

**Bryan D. Young, MD PhD, FACC**
Assistant Professor of Medicine
Division of Cardiovascular Medicine, Department of Internal Medicine
Yale School of Medicine; Yale New-Haven Health System
New Haven, Connecticut

*This page intentionally left blank*

# PREFACE

We are pleased to present this fourth edition of *Nuclear Cardiology: Practical Applications*. We have undertaken substantial revisions, emphasizing recent changes in technology as well as the contemporary clinical applications of nuclear cardiology. We have provided insight as to future directions of the field, delineating where this important imaging modality is positioned in current-day clinical practice, especially in the setting of multi-modality imaging. We have greatly expanded information regarding positron emission tomography, including an entire chapter on the assessment of myocardial blood flow. Each chapter now features a table of key points and many of the tables and figures have been updated and expanded. We believe these help in the learning process as well as providing easy referencing key pieces of information. For your personal knowledge assessment, especially for preparation for credentialing examinations, we have provided a multitude of questions with detailed answers related to each chapter, found at the end of the book.

This fourth edition is ideally suited for trainees and early-career professionals both radiologists and cardiologists. Additionally, this book should be very useful for technologists and healthcare professionals involved in decision-making for testing procedures.

We are grateful to the contributors who have done an outstanding job updating and expanding the book and its value. We hope that you find the fourth edition of *Nuclear Cardiology: Practical Applications* useful and that it will be a focal point for your nuclear cardiology education. To this end, it is our goal to assist in the improvement of nuclear cardiology practice and to benefit the patients for which we care.

Gary V. Heller
Robert C. Hendel

*This page intentionally left blank*

SECTION

# 1

# FUNDAMENTALS OF NUCLEAR CARDIOLOGY

*This page intentionally left blank*

# Fundamentals of Nuclear Cardiology Physics

CHAPTER 1

C. David Cooke, James R. Galt and E. Lindsey Tauxe

## KEY POINTS

- Elements are defined by the number of protons in the nucleus. Nuclides are defined by the number of protons and the number of neutrons.
- The ratio of protons to neutrons determines the stability of a nucleus.
- Unstable nuclei decay to a more stable state through several different mechanisms: $\alpha$ decay, $\beta^-$ decay, $\beta^+$ (positron) decay, electron capture, and isomeric transition.
- The rate at which unstable nuclei decay can be described by the decay constant. It is often more convenient to describe the rate of decay by the half-life.
- The interaction of radiation with matter is dependent on the energy and type of the radiation, as well as the atomic number ($Z$ number) of the matter.
- Attenuation is the loss of radiation as it passes through matter and is absorbed or deflected.

## INTRODUCTION

A practical review of basic atomic and nuclear physics is essential to understand the origins of radiations, as well as their interactions with matter. The nature and type of emissions are determined by the structural character of the atom and nucleus. The ways in which radiation interacts with matter have a direct relationship with imaging and radiation safety. The types of radiations and the ways in which they interact with matter are the foundation of radionuclide imaging and radiation safety. This chapter will focus on atomic and nuclear structure and the interaction of radiations with matter as they relate to radionuclide imaging.

## ATOMIC AND NUCLEAR STRUCTURE

Matter is composed of atoms and the characteristics of a specific form of matter are determined by the number and type of atoms that make it up. How atoms combine is a function of their electron structure. The electron structure is determined by the nuclear architecture. As we have yet to image the atom, its structure is based on a "most-probable" model that fits physical behaviors we observe. The probabilistic approach is based on the model of the atom proposed by Niels Bohr in 1913. The Bohr atom proposed a positively charged nucleus, surrounded by negatively charged electrons. A neutral atom is one in which the positive and negative charges are matched. A mismatch in these charges determines the ionic character of the atom, which is the basis for its chemistry. The electron configuration is also a source for emissions used in radionuclide imaging.

These emissions, or *radiations*, will be in one of two forms: particulate or electromagnetic. The

origins of either type of radiation may be from the nucleus or the electron structure.

## Electron Configuration

Electrons are arranged around the nucleus in shells. The number of shells is determined by the number of electrons, which is, in turn, determined by the number of protons in the nucleus. The force exerted on these shells, called *binding energy*, is determined by the proximity of the shell to the nucleus. Higher binding energies are exerted on shells closest to the nucleus and conversely, lower binding energies for those more distant from the nucleus. The innermost shell is named the "K" shell and electrons in this shell are subject to the highest binding energy. The magnitude of that energy is dependent on the positive forces, which is determined by the number of protons in the nucleus. The shells more distant from the nucleus are named L, M, N, and so on. Each of these shells has lower binding energies as a result of their distance from the nucleus (Fig. 1-1).

The radii of each of these shells increase as a function of their distance from the nucleus. An expression of this is given by assigning an integer value (1, 2, 3, …) to each shell. The lower values represent smaller radii. These integer values are called *quantum numbers*. Therefore, the K shell has a quantum number of 1, L = 2, M = 3, etc. This pattern continues until all available electrons are bound to a shell. The innermost shells are filled with electrons preferentially. The maximum number of electrons is specific to each shell and is calculated by $2n^2$, where $n$ is the *quantum number*. Therefore, the maximum number of electrons for each shell is:

$$\text{K} = \text{quantum \#1} = 2(1)^2 = 2 \text{ electrons}$$
$$\text{L} = \text{quantum \#2} = 2(2)^2 = 8 \text{ electrons}$$
$$\text{M} = \text{quantum \#3} = 2(3)^2 = 18 \text{ electrons}$$

These shells are further subdivided into *substates*. The number of *substates* for each shell can be calculated by $2n - 1$; therefore:

$$\text{K shell} = 2(1) - 1 = 1 \text{ substate}$$
$$\text{L shell} = 2(2) - 1 = 3 \text{ substates}$$
$$\text{M shell} = 2(3) - 1 = 5 \text{ substates}$$

Each substate for a given shell will have a unique binding energy. For instance, the L shell has three substates, $L_I$, $L_{II}$, and $L_{III}$.[1] Each of these has slightly different distances from the nucleus, and therefore slightly different binding energies (Fig. 1-2).[2]

### Atomic Radiations

Electrons in inner shells being under high binding energy and thus tightly bound to the nucleus are in an inherently low-energy state. Outer shell and free electrons are in an inherently higher-energy state. Therefore, to move an inner shell electron to an outer shell *requires* energy. The amount of energy required is simply the difference between binding energies.

Example: Binding energy for a hypothetical "K" shell = 100 keV and "L" = 50 keV. $K_{100} - L_{50} = 50$ keV

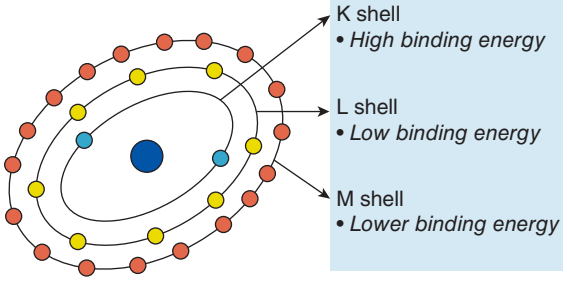


**FIGURE 1-1** Atomic structure. The nucleus is surrounded by electron shells. The binding energy decreases as the distance from the nucleus increases (K > L > M).

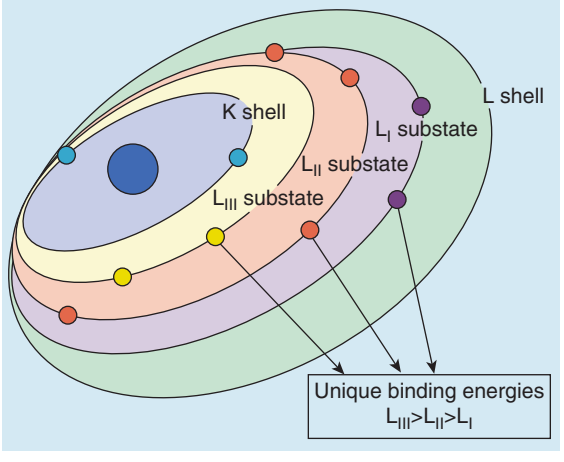


**FIGURE 1-2** Electron configuration. Electrons are arranged in subshells, as illustrated for the L shell. Each subshell has a unique binding energy.

of energy *input* to move the electron from the "K" shell to the "L" shell.

Conversely, the movement of an electron from an outer shell to an inner shell, L → K, yields energy. This energy yield results in the emission of radiation. The energy of the radiation is equal to the differences in binding energies of the shells. The radiation may take on two different forms: characteristic x-ray or Auger (oh-zhay) effect.

Example: Binding energy for a hypothetical "K" shell = 100 keV and "L" = 50 keV. $K_{100} - L_{50} =$ 50 keV of energy *released* as the electron moves from the "L" shell to the "K" shell.

Characteristic x-rays are electromagnetic radiations (photons) that are created when an outer shell electron moves to fill an inner shell vacancy. This vacancy may occur for several reasons—to be discussed later. The energy of this photon is equal to the difference between binding energies. Since binding energies are determined by, or characteristic of, the number of protons in the nucleus, and it is the number of protons that determines an element's identity, the characteristic x-ray energies are specific to each element and the electron shells from which they originate. X-radiation is defined as an electromagnetic radiation originating outside the nucleus, therefore the term characteristic x-ray.

The Auger effect occurs under the same conditions as characteristic x-ray, that is, an inner shell vacancy being filled by an outer shell electron. The difference is that the excess energy from the cascading electron is radiated to another electron. This ejects that electron from its shell. This free electron will have kinetic energy equal to the difference in the binding energies less the binding energy of the shell of the free electron. The Auger effect is more common in elements with lower numbers of protons ($Z$ number).[1–3]

## Nuclear Structure

The nucleus is composed mainly of neutrons and protons. Any particle contributing to the structure of the nucleus is called a *nucleon*. The conventional nomenclature to describe the nucleons is: ${}^{A}_{Z}X_{N}$.

where:

X = Symbol of the chemical element
$A$ (Atomic mass number) = Total number of nucleons = # Protons + # Neutrons
$Z$ (Atomic number) = # Protons
$N$ = # Neutrons

Since the number of neutrons ($N$) can be derived from the atomic mass number ($A$) and the number of protons ($Z$), it is usually omitted ($N = A - Z$). In addition, since the number of protons ($Z$) defines an element, as does its chemical symbol ($X$), only one is necessary; hence, $Z$ is often omitted as well.

The total mass of an atom is essentially the combined masses of the nucleons. Electrons contribute less than 1% to the total mass.[1]

Nuclides having the same number of protons ($Z$) are called *isotopes*. Isotopes are the same element, but have different atomic masses ($A$) and therefore have different numbers of neutrons ($N$); for example: ${}^{125}_{53}I_{72}$, ${}^{127}_{53}I_{74}$, and ${}^{131}_{53}I_{78}$. Nuclides with the same number of neutrons ($N$) are called *isotones* and will be different elements, since the number of protons ($Z$) will be different; for example: ${}^{131}_{53}I_{78}$, ${}^{132}_{54}Xe_{78}$, and ${}^{133}_{55}Cs_{78}$. Nuclides with the same atomic mass number ($A$) are called *isobars* and are different elements as well, since they will have different numbers of protons ($Z$) and neutrons ($N$); for example: ${}^{99}_{42}Mo_{57}$ and ${}^{99}_{43}Tc_{56}$. Finally, nuclides with the same number of protons ($Z$) and neutrons ($N$), but in different energy states are called isomers; for example: ${}^{99m}_{43}Tc$ and ${}^{99}_{43}Tc$. An easy mnemonic for remembering this is that isotopes (with a **p**) have the same number of **p**rotons, isotones (with an **n**) have the same number of **n**eutrons, isobars (with an **a**) have the same **a**tomic number, and isomers (with an **e**) are the same nuclide with different **e**nergies.

Isotopes having different $N$ numbers are of particular interest to imagers because they have the same chemistry, since their $Z$ numbers and, therefore, electron numbers are the same.[1–5] Some isotopes exhibit the emission of radiations, which is due to the differences in the number of neutrons. These isotopes are called *unstable*. If all the stable isotopes of all elements are plotted, comparing proton number to neutron number, a pattern emerges as illustrated in Figure 1-3.

Elements with low $Z$ numbers have proton to neutron ratios that are 1:1. As $Z$ numbers increase, this ratio increases to as high as 1.5. This distribution of stable elements is called the *line of stability*. By definition, an element with a proton to neutron ratio that falls to either the left or right of the *line of*

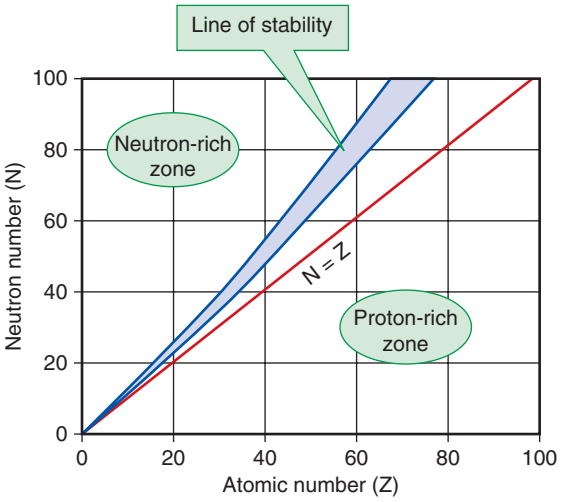


**FIGURE 1-3** Line of stability. All naturally occurring stable nuclides fall along a distribution known as the line of stability (LOS). As illustrated, for light elements ($Z < 20$) $N \sim Z$ and for heavier elements $N \sim 1.5Z$. Unstable elements, lying to the left of the LOS, are neutron rich; those lying to the right of the LOS are proton rich.

*stability* is unstable. The unstable isotopes, *radioisotopes*, are unstable because their nuclear configurations are either proton rich or neutron rich relative to stable configurations. These radioactive elements seek stability by undergoing transformations in their nuclear configurations to a more stable P ↔ N ratio. The type of transformation will be a result of the P ↔ N ratio, that is, proton rich versus neutron rich. This type of transition is called the mode of decay.[1–4]

### *Modes of Decay*

The goal of nuclear decay is to equate the balance of forces in the nucleus. The repelling forces originating from the positive charge (*coulombic forces*) of the protons, when matched by the attractive forces from within the nucleus (*exchange forces*), define **stability**. When these forces are mismatched, nuclear transformations (*radioactive decay*) result. The mode of decay will produce unique emissions and lead to a more stable nuclear configuration. In radionuclide imaging, the ideal mode of decay would result in a high yield of photons, at an energy that is efficiently detected by our imaging instrumentation. Photon emission is also desirable from the radiation safety and dosimetry perspectives, due to their lower probability of creating potentially damaging interactions as compared to particles. With these considerations, it is important to understand the modes of decay of $^{99m}$Technetium, $^{201}$Thallium, and $^{82}$Rubidium—the most commonly used radionuclides in nuclear cardiology.[1,2]

#### $\beta^-$ Decay

In an unstable nuclear configuration where the nucleus is neutron rich, $\beta^-$ decay occurs. To decrease the neutron–proton ratio, a neutron is converted to a proton and an energized electron is emitted. The expression of this nuclear transition is:

$$n \rightarrow p + e^- + \nu + \text{energy}$$

where n is the neutron, p the proton, e the electron, and ν is the neutrino.

The neutrino (ν) behaves like a particle with no mass and is not critical to imaging considerations. The primary emission is the energized electron ($e^-$). The nuclear configuration that results from $\beta^-$ decay is a *daughter* with a stable or more stable energy state and an additional proton in its nucleus.

Example: $^{14}_{6}C_8 \rightarrow {}^{14}_{7}N_7$

Since the number of protons is changed, the elemental identity changes. This is called a transmutation. The daughter atomic mass ($A$) remains the same as the parent nucleus, and the energy carried off by the ejected electron is called transition energy. This leads to a more balanced relationship of coulombic force (repelling forces due to the protons) and exchange force (attractive nuclear forces). The resulting emission of the energized electron, a $\beta^-$ particle, is of no use in imaging and contributes to an increase in radiation dose in a biologic system. This decay process may lead to a daughter that is not fully stable, but more stable than the parent.[1,2] The change in nuclear configuration is an increase in $Z$ and a decrease in $N$.

#### $\beta^+$ Decay

In nuclear configurations where the *parent* is proton rich, $\beta^+$ decay may occur. In this mode of decay, a proton is converted to a neutron and the emission of

an energized, positively charged electron ($\beta^+$) results. The nuclear equation is:

$$p \rightarrow n + e^+ + \nu + \text{energy}$$

The energy of the $\beta^+$ particle contributes to resolving the *transition energy* between the unstable parent and more stable daughter, as in $\beta^-$ decay.

An important secondary emission will result from the formation of the $\beta^+$ particle. Since there is an abundance of negatively charged electrons in nature, the resulting positively charged electron ($\beta^+$) will be attracted to, and collide with, a free negatively charged electron. This collision results in the *annihilation* of both particles. The annihilation leads to the conversion of the mass of these particles to their equivalent energy state. This is expressed by Einstein's equation $E = mc^2$, where $E$ is energy, $m$ the mass, and $c$ is the speed of light. This essentially states that energy and mass are simply two physical forms of the same thing. Therefore, two photons ($E$) are emitted, each with the energy equivalent to the mass ($m$) of an electron, which is 511 keV. Unique to this annihilation is that these photons are emitted in a 180-degree trajectory from each other. It is these photons that are detected and registered into an image in positron imaging, such as with $^{82}$Rb. The change in nuclear configuration is a decrease in $Z$ and an increase in $N$.

Example: $^{82}_{37}Rb_{45} \rightarrow {}^{82}_{36}Kr_{46}$

### Electron Capture

An alternative to $\beta^+$ decay in proton-rich nuclear configuration is *electron capture*. This mode of decay is defined as the capture of a K-shell electron by the nucleus, the subsequent combination with a proton, and creation of a neutron. The nuclear expression is therefore:

$$p + e^- \rightarrow n + \nu + \text{energy}$$

The vacancy left by the captured electron would then be filled by an outer shell electron. A cascade of an electron, filling subsequent vacancies, creates secondary emissions called *characteristic x-rays* and *Auger electrons*. The energies of these emissions will be characteristic of the binding energy of the daughter, since the nuclear transition occurred prior to the production of the x-rays and Auger electrons. It is the *characteristic x-rays* that are imaged in $^{201}$Tl myocardial perfusion imaging. The energy of the x-rays is determined by the binding energy of $^{201}$Hg, the daughter of the decay of $^{201}$Tl. Electron capture decreases the proton–neutron ratio.[1]

Example: $^{201}_{81}Tl_{120} \rightarrow {}^{201}_{80}Hg_{121}$

### Isomeric Transitions and Internal Conversions

The daughter of the decay of a radioactive parent will ideally be in its most stable energy configuration or *ground state*. This does not always occur, leading to either of the two unstable states: *excited state* or *metastable state*. Excited states are very unstable and exist for very short time periods, usually less than $10^{-12}$ seconds. Metastable states, however, may exist for several hours. These metastable states lead to the release of energy in the form of electromagnetic emissions, without changing the proton–neutron ratios. The daughter nucleus has the same nuclear structure as the parent has, but in a more stable energy configuration. This form of decay is called an *isomeric transition* and results in electromagnetic emissions called $\gamma$-*rays*. These emissions are the same as x-rays, differing only by their location of origin, that is, the nucleus. As noted with the production of characteristic x-rays, there is a competing process, resulting in a particulate radiation. This process is called *internal conversion*. For any given metastable state, there is a specific ratio of *isomeric transitions* to *internal conversions*. In imaging, the higher percentage of isomeric transitions compared to internal conversions is preferred due to the resulting higher yield of photons. The decay of $^{99m}$Tc to $^{99}$Tc is an example of an isomeric transition of the metastable state ($^{99m}$Tc). The percent occurrence of isomeric transitions of a population of $^{99m}$Tc nuclei is approximately 87%. For example, for every 100 decays of $^{99m}$Tc nuclei, there is a yield of 87 $\gamma$-photons and 13 internal conversion electrons.

For any given mode of decay, should the daughter be metastable, there will be the emission of $\gamma$-photons and internal conversion electrons as secondary emissions. This will be indicated as [$B^-$, $\gamma$], [$B^+$, $\gamma$], [EC, $\gamma$], and so forth. The internal conversion electron

yield, in ratio to γ-photon yield, is specific to a given radionuclide.[1,2,5]

### Alpha (α) Decay

In unstable nuclei with very high atomic masses, the most probable mode of decay is α decay. An alpha particle consists of two protons and two neurons, which is essentially a helium nucleus. Alpha decay results in a daughter with a *Z* number of 2 less than the parent and an atomic mass less by 4 relative to the parent.

Example: $^{235}_{92}U_{143} \rightarrow {}^{231}_{90}Th_{141}$

Due to its high charges and heavy mass, the alpha particle has a very short travel distance in matter and deposits its energy very quickly. It has no application in diagnostic imaging and induces significant potential for biologic damage.[1,3]

### *Decay Schemes*

The modes of decay may be expressed graphically, called *decay schemes*. Decay schemes graphically illustrate all possible nuclear transitions that unstable nuclei undergo. They are often accompanied by tables with detailed information about the transitions, such as the percentage occurrence, isomeric transitions, internal conversions, characteristic x-rays, Auger electrons, and biologic dose information.

In decay schemes, the nuclear energy levels are expressed as horizontal lines. The space between these lines represents the *transition energy (Q)*.

The types of emissions are depicted by a unique direction of a line (Fig. 1-4).

Note that the arrows may be angled to either the right or left. In neutron-rich parents, the mode of decay "shifts" the daughter to the right, corresponding to the shift on to the line of stability graph. Conversely, a mode of decay for a proton-rich parent moves to the left, toward the line of stability.

The tables that accompany decay schemes provide additional detail including the secondary emissions, as mentioned earlier. Since many of the secondary emissions are particulate, that is, electrons, these data are of particular interest in radiation dosimetry. In the decay scheme for $^{201}$Tl, the data regarding the characteristic x-rays of $^{201}$Hg are in these tables.

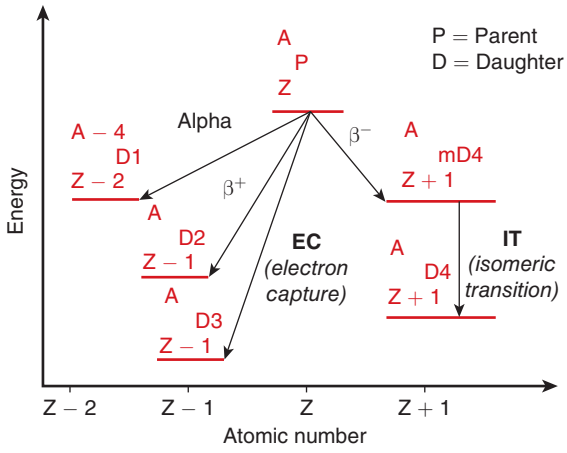


**FIGURE 1-4** Decay schemes. This figure illustrates the configurations of decay schemes for the different modes of decay. The schemes move to the left for proton-rich radionuclides and to the right for neutron-rich radionuclides.

### *Parent–Daughter Equilibrium*

Not all nuclear transitions lead to a stable daughter. The β⁻ decay of $^{99}$Mo yields $^{99m}$Tc, which then decays to $^{99}$Tc by *isomeric transitions* and *internal conversions*. $^{99m}$Tc decays to $^{99}$Tc with an 87% frequency through isomeric transitions. Therefore, for every 100 decays of $^{99m}$Tc, we observe 87 γ-rays and 13 internal conversion electrons, as stated earlier. This higher yield of photons makes $^{99m}$Tc a very desirable radionuclide for imaging. A sample of $^{99}$Mo would always contain some proportion of $^{99m}$Tc and $^{99}$Tc. Since both parent and daughter are decaying, the relative activities would reach equilibrium, based on their half-lives. These states of equilibrium are employed when using both technetium and rubidium generators. When the parent half-life is marginally longer than that of the daughter, the amount of the daughter in the mixture will reach a maximum over a period of time. That elapsed time will be a multiple of half-lives of the daughter. If the daughter radionuclide is removed from the mixture, the same multiple of half-lives will have to occur, before the maximum amount of the daughter is subsequently reached. This equilibrium state is called *transient equilibrium*.[2,4] It is this transient state that is the basis of $^{99m}$Tc production from $^{99}$Mo–$^{99m}$Tc generators (Fig. 1-5).

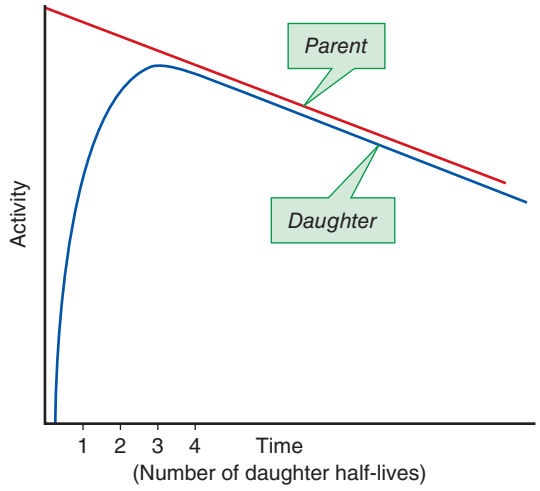


**FIGURE 1-5** Transient equilibrium. When the parent half-life is marginally longer than that of the daughter, the amount of daughter activity will reach a maximum after relatively few daughter half-lives have passed. $^{99}$Mo and $^{99m}$Tc typically reach transient equilibrium after approximately four $^{99m}$Tc half-lives.

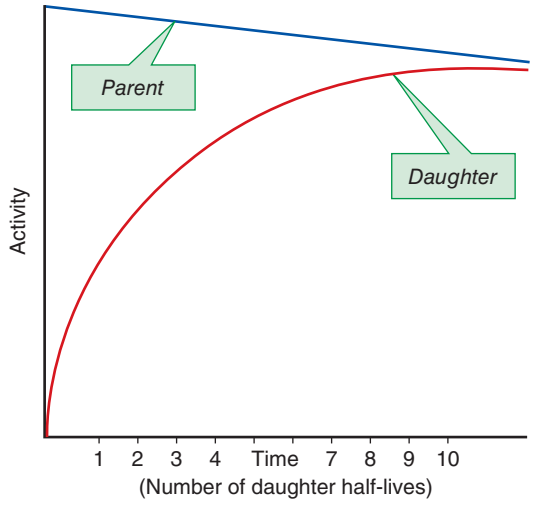


**FIGURE 1-6** Secular equilibrium. When the parent half-life is considerably longer than that of the daughter, the amount of parent activity will decrease very little over time. Therefore, many more daughter half-lives must pass before the equilibrium is reached. An example is $^{82}$Sr with a half-life of 25 days and $^{82}$Rb with a 1.2-minute half-life.

In parent–daughter mixtures where the half-life of the parent is markedly longer than that of the daughter, *secular equilibrium* is reached. In this state of equilibrium, the concentration of the parent is decreasing so slowly relative to the daughter that the mixture appears to have the half-life of the parent. It is this equilibrium that is the basis for the $^{82}$Sr–$^{82}$Rb generators used in $^{82}$Rb positron emission tomography (PET) imaging (Fig. 1-6).[1]

## RADIOACTIVITY

The specific time that an unstable nucleus will undergo a transition cannot be determined, only *predicted*. Nuclear transitions are spontaneous and random, so the mathematics of radioactive decay is based on probabilities and rates, not specific nuclear events. If a population of radioactive atoms, $N$, is considered, the rate of nuclear transitions would be expressed as $\Delta N/\Delta t$. The rate implies that a constant would express the average number of transitions that occur per unit time. This constant is called the *decay constant*; which is specific to a given radionuclide and is expressed as $\lambda$. The mathematical relationship is: $\Delta N/\Delta t = -\lambda N$, where $N$ is the total number of radioactive nuclei and $\lambda$ the decay constant. Since the total $N$ decreases with time ($t$), the decay constant ($\lambda$) is a negative value.[1,2,4] The number of transitions per unit time ($\Delta N/\Delta t$) is called *activity*. Activity is measured in curies (Ci), which is defined as $3.7 \times 10^{10}$ disintegrations per second (dps). The International System of Units (SI) unit equivalent is the becquerel (Bq), which is defined as 1 Bq = 1 dps. So 1 Ci = $3.7 \times 10^{10}$ Bq. The most commonly used units are in the mCi (MBq) range for nuclear cardiology procedures.

In nuclear decay, the number of radioactive nuclei ($N$) is always decreasing as time passes at an average rate defined by the decay constant ($\lambda$). Decay is expressed, therefore, as an exponential function; that is, the number of radioactive nuclei available is affected by both the number of unstable nuclei and its average rate of decay. To calculate the specific number of decays for a given time, we have the following expression:

$$N_{(t)} = N_{(0)}\, e^{-\lambda t}$$

where $N_{(t)}$ is the number of unstable nuclei remaining after the elapsed time ($t$) has passed. The expression